Torsional Stiffness Testing and Analysis of Composite Doublewedge Rocket Fins

Parth Garud* and Robert Ajluni†
Georgia Institute of Technology, Atlanta, GA, 30332

Composite sounding rocket fins offer a lightweight and high-strength solution to vehicle stability. However, accurately modeling and characterizing these composites can prove challenging due to their anisotropic properties and the dynamic and extreme conditions experienced during rocket launches. Thus, sophisticated analyses to ensure reliable performance predictions are necessary. This paper presents a novel method to experimentally determine the torsional stiffness of composite fins for a sounding rocket, as well as a comparison of the experimental results to a finite element model. This test was developed to characterize fins on vehicles built by Georgia Tech Experimental Rocketry, a project team of the Ramblin' Rocket Club (RRC) at Georgia Tech, to aid in analyzing aeroelastic flutter. The test article was composed of a carbon fiber layup on a Formlabs Rigid-10K additively manufactured core attached to a representative model airframe with a tip-to-tip layup. The fins were then twisted on an Instron load frame about the vehicle's appropriate radial axis to determine their torsional stiffness. The geometry, composition, and manufacturing of the fins pose a unique challenge for their modeling. The ability to vet this modeling approach with experimental data for a subset of fins is crucial to building confidence in accurately modeling a larger variety of fin geometries. Furthermore, the results obtained from the experiment can be used to estimate aeroelastic flutter for composite fins.

I. Nomenclature

A	=	square shaft cross-sectional area, in^2
F	=	vertical force applied by the load frame, lb_f
JG	=	torsional stiffness, $lb_f in^2$
L_c	=	clamp length, in
T	=	torque applied on the shaft, $lb_f in$
T_r	=	torque component in the radial direction, $lb_f in$
c_r	=	root chord, in
c_t	=	tip chord, in
d_p	=	pitch diameter, in
s	=	fin semi-span, in
y	=	vertical loadframe displacement, in
Δr	=	radial difference in clamp endpoints, in
δ_t	=	maximum vertical fin tip displacement, in
ϕ_s	=	shaft angle of twist, rad

*Undergraduate Student, School of Aerospace Engineering, pgarud3@gatech.edu, AIAA University Student Member .
†Undergraduate Student, School of Aerospace Engineering, rajluni3@gatech.edu, AIAA University Student Member .

II. Introduction

Composite sandwich panels have emerged as crucial components in numerous aerospace applications due to their exceptional strength-to-weight ratio, offering unparalleled advantages in various structural configurations. These panels find extensive utilization in critical components such as fins[1, 2], wings[3], and turbomachinery[4, 5], where their ability to withstand high torsional loads is of paramount importance. The lightweight yet durable nature of composite sandwich panels makes them ideal for enhancing overall performance while adhering to stringent weight restrictions imposed in aerospace design.

In the domain of supersonic rocketry, the phenomenon of fin flutter presents significant challenges in ensuring the stability and reliability of aerospace vehicles. Flutter, characterized by self-sustained oscillations of structures under aerodynamic loads, underscores the need for precise characterization of composite materials, particularly their torsional stiffness about the radial axis, to mitigate potential instabilities[6, 7]. Understanding the complex interplay between aerodynamic forces and structural dynamics is essential for predicting and preventing detrimental effects such as flutter, which can compromise the integrity and performance of aerospace systems.

While classical lamination theory provides a fundamental framework for estimating the properties of composite structures[8], its applicability diminishes for complex geometries encountered in aerospace applications[9, 10]. Consequently, experimental validation becomes indispensable to verify the accuracy of modeling techniques and simulation capabilities[11–13]. By conducting rigorous experimental testing on composite sandwich panels with varying geometries and material compositions, researchers can refine finite element models and computational simulations, ensuring their fidelity in predicting real-world behavior under diverse operating conditions.

To address these challenges, this paper presents a novel experimental approach aimed at determining the torsional stiffness of composite fins for sounding rockets about the radial axis. This approach was developed by students at Georgia Tech Experimental Rocketry (GTXR), a project team of the Ramblin' Rocket Club at Georgia Tech. Unlike previous studies focusing on flat plates[14], our research investigates swept structures with varying chordwise and spanwise thicknesses, which are more representative of actual hardware flown by GTXR. This innovative approach allows for a more accurate assessment of torsional stiffness under real-world conditions, providing valuable insights into the structural integrity and performance of composite materials in sounding rocket applications.

Moreover, our study conducts a comprehensive comparison between modeled and experimental data, providing valuable insights into the fidelity of modeling techniques and simulation capabilities in replicating real-world behavior. By conducting a comparison between simulated and experimental data, this study advances our understanding of composite material behavior and enhances the accuracy of predictive models for different failure modes. Through analysis and validation of computational models, researchers can optimize the design and performance of composite structures, ensuring their reliability and safety in demanding flight environments.

Crucially, the validated modeling techniques alleviate the need for extensive physical testing on each individual design, thereby mitigating the risk of damaging flight hardware and streamlining the design iteration process. Through the prudent application of finite element analysis, we can confidently predict the behavior of composite structures and optimize their performance with precision.

In summary, this paper investigates the torsional stiffness of composite fins for sounding rockets, highlighting the critical role of accurate characterization and validated modeling techniques in ensuring the safety and efficacy of these structures. By leveraging experimental data and computational simulations, the challenges posed by complex material behavior and aerodynamic phenomena can be overcome.

III. Experimental Methods

A. Test Article

A test fin-can was designed and built to conduct the experiment. This test article consisted of 4 fins of identical dimensions. Each fin had a symmetrical double-wedge airfoil and was composed of an additively manufactured core material with a carbon fiber layup. The article was manufactured in two phases: a sandwich layup to construct the fins and a tip-to-tip layup to attach them to the tube. Two different materials were used to print the fin cores: Formlabs™ Rigid 10K and High Temp resins. Fibreglast™ Prepreg 3K, 2x2 Twill Weave Carbon was used for all the reinforcing layups. The relevant material properties for all can be found in Tables 1 and 2.

The fins were made with geometric proportions similar to previous fin geometries flown by GTXR[15]. This was done to ensure that the data gathered would not deviate from flight hardware due to unforeseen geometric effects. The final fin design, shown in Fig. 1 and Table 3, was chosen due to its similarity to flight geometries and manufacturing

Property	Value	Unit
Density	1.16	g/cm^3
Young's Modulus	10.0	GPa
Poisson's Ratio	0.36	-
Shear Modulus	3.67	GPa

Table 1 Material properties for Formlabs Rigid 10K Resin.

Property	Value	Unit
Density	1.42	g/cm^3
In-plane Young's Modulus	61.34	GPa
Out-of-plane Young's Modulus	6.9	GPa
In-plane Poisson's Ratio	0.3	-
Out-of-plane Poisson's Ratio	0.04	-
In-plane Shear Modulus	2.7	GPa
Out-of-plane Shear Modulus	3.3	GPa

Table 2 Material properties for epoxy carbon fiber woven (230GPa) pre-preg.

constraints. Once the fin cores had been 3D-printed, three Rigid 10K fins and one High Temp fin were selected to be the test fins. Rigid 10K fins were preferred because the High Temp fins showed signs of warping. A warp at the root of the High Temp fins made it difficult to bond the fins onto the test airframe. The High Temp fins also had cracks due to thermal expansion during the curing process. While the Rigid 10K fins were more brittle and thus more prone to chip at the edges, they were selected for their better dimensional stability.

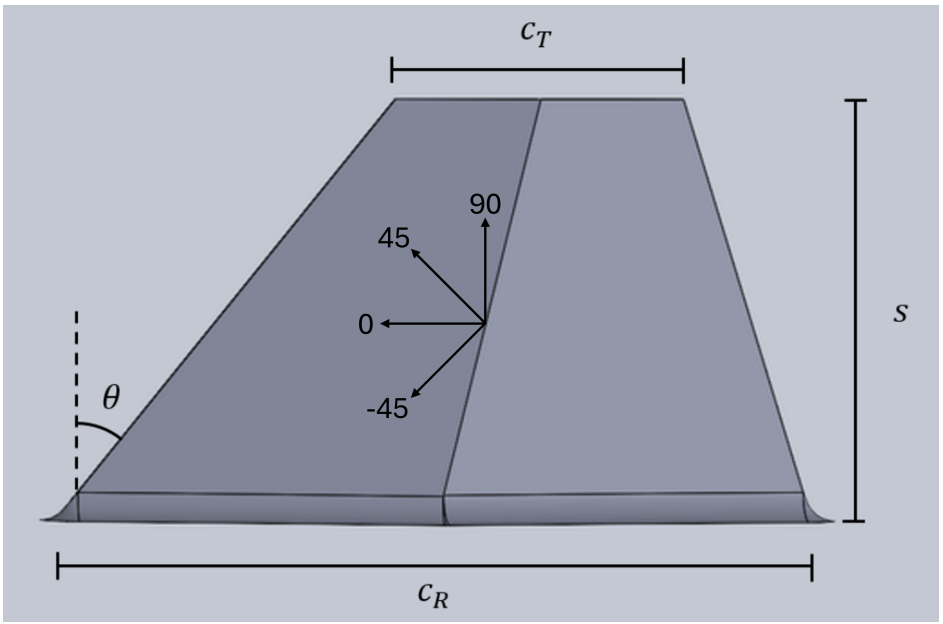

Fig. 1 A computer-aided design of the test fin core

Dimension	Value	Unit
Root Chord (c_R)	7.13	in
Tip Chord (c_T)	2.78	in
Root Thickness (max) (t_R)	0.48	in
Tip Thickness (max) (t_T)	0.20	in
Span (s)	4.00	in
Sweep (θ)	38.6	$degrees$

Table 3 Test fin core dimensions

These fins were used as a core material in a quasi-isotropic carbon fiber layup to make the fin sandwich panels. The sandwich panel fins were bonded to the airframe body and an additional layup was done to securely attach them. The plies of this layup spanned from the tip of one fin to the tip of the adjacent fin. While this tip-to-tip layup was conducted, two of the bonded fins detached from the airframe. These fins were reattached, but due to the nature of the airframe mounting during the layup, an optimal bond could not be made. The full ply stack, including both the sandwich layup as well as the tip-to-tip layup, can be seen in Fig. 2 and Table 4. Additional information and clamping dimensions are shown in Table 5

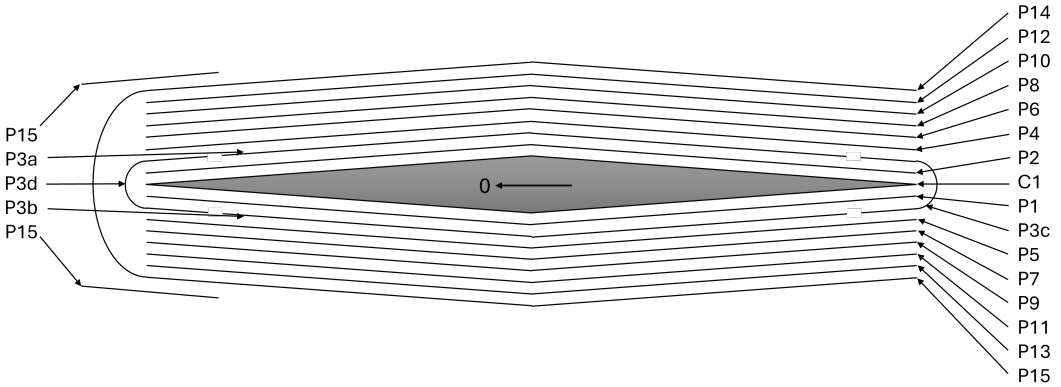

Fig. 2 Ply buildup of the test fins with the sandwich (P1-P5) and tip-to-tip (P6-15) layups.

Ply	Material	Orientation	Thickness	Step
C1	Formlabs Rigid 10k Resin	N/A	N/A	1
P1	Fibreglast Prepreg 3K	30/-60	0.012	2
P2	Fibreglast Prepreg 3K	30/-60	0.012	3
P3a	Fibreglast Prepreg 3K	60/-30	0.012	4
P3b	Fibreglast Prepreg 3K	60/-30	0.012	5
P3c	Fibreglast Prepreg 3K	45/-45	0.012	6
P3d	Fibreglast Prepreg 3K	45/-45	0.012	7
P4	Fibreglast Prepreg 3K	0/90	0.012	8
P5	Fibreglast Prepreg 3K	0/90	0.012	9
P6	Fibreglast Prepreg 3K	0/90	0.012	10
P7	Fibreglast Prepreg 3K	0/90	0.012	11
P8	Fibreglast Prepreg 3K	45/-45	0.012	12
P9	Fibreglast Prepreg 3K	45/-45	0.012	13
P10	Fibreglast Prepreg 3K	0/90	0.012	14
P11	Fibreglast Prepreg 3K	0/90	0.012	15
P12	Fibreglast Prepreg 3K	45/-45	0.012	16
P13	Fibreglast Prepreg 3K	45/-45	0.012	17
P14	Fibreglast Prepreg 3K	82.6/-7.4	0.012	18
P15	Fibreglast Prepreg 3K	45/-45	0.012	19

Table 4 Ply stack-up for test fin build up shown in Fig. 2

Fin	Material	Azimuth	Δr	L_c	Notes
1	Rigid 10K	90	0.375	12	Reattached during tip-to-tip layup
2	High Temp	180	0.125	12	Minor cracking and warping
3	Rigid 10K	270	0.0625	12	Reattached during tip-to-tip layup
4	Rigid 10K	0	0	12	No defects
ANSYS	Rigid 10K	N/A	0	N/A	Finite element model

Table 5 Test fin locations and information

B. Test Fixture

The test fixture designed for this experiment transferred vertical compression of the load frame to radial torsion of the test fin. The force applied by the load frame was transferred to a torque by using a rack and pinion mechanism. As the load frame displaces the rack downwards, the pinion gear is rotated in the positive radial direction of the fin. The shaft turned by the pinion is welded to a clamping mechanism that clamps to the tip chord of the test fin. A schematic of the test fixture is shown in Fig. 4(a).

Achieving secure mating between a clamp and the test fin was difficult, as the surface was at a compound angle. For the swept fins we were testing, the surface is inclined with respect to both the radial and axes. To tackle this issue, we explored two distinct approaches, pictured in Fig. 3. Firstly, we utilized 3D printing technology to fabricate the negative shape of each side of the fin tip, subsequently affixing it to flat plates via bonding. These flat plates were then maneuvered along all-thread rods to adjust their positioning and clamp them onto the fin. Alternatively, a machining-based strategy was pursued, where small aluminum blocks were set at the compound angle and milled to the correct height. These aluminum blocks were then fastened to the flat plates via screws, enabling us to employ the same clamping methodology as in the preceding method. Through these approaches, we endeavored to establish effective clamping mechanisms that accommodated the geometry of the test fins. The 3D printed clamps were chosen for their larger contact area with the fin (Fig. 4(c)), with the machined clamps kept as backups in the event that the 3D prints began to crack when loaded.

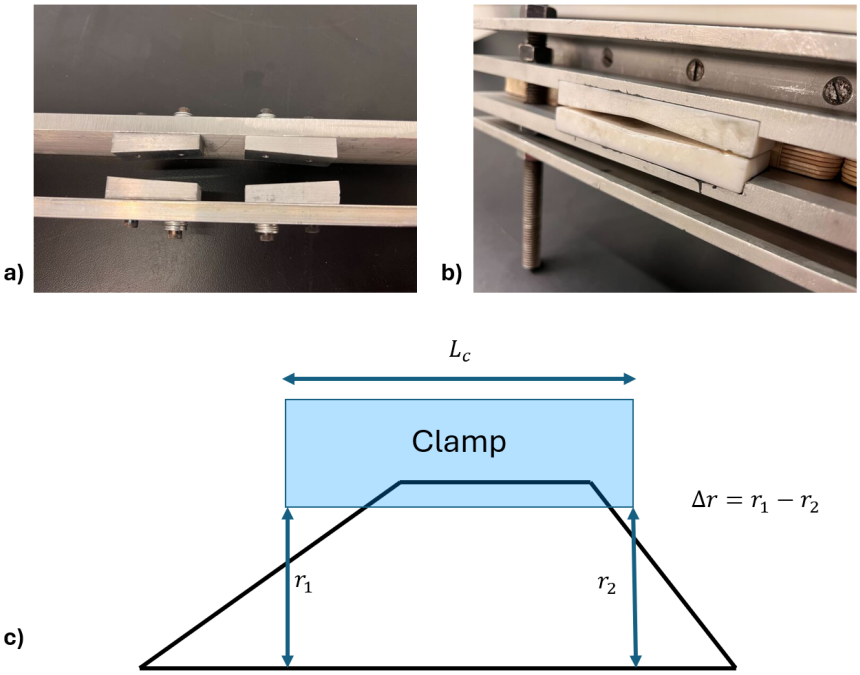

Fig. 3 a) The machined fin clamp and b) the 3D-printed fin clamp, and c) relevant measured dimensions once fins were clamped.

The test airframe was mounted to the load frame using custom machined T-brackets. The brackets were affixed to the load frame and the airframe was secured to the brackets with heavy-duty hose clamps. The brackets were positioned such that they would take the bending load of the article and the hose clamps were only needed to prevent axial motion and hold the weight of the article when it was unloaded. An image of the full setup is shown in Fig. 4(b).

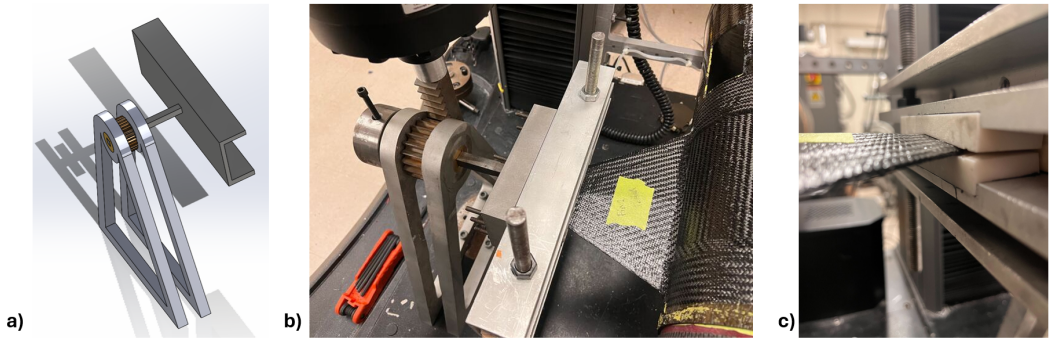

Fig. 4 a) A concept illustration of the load transfer mechanism, b) The full test setup with the test article attached, and c) the clamping interface between the test fin and the load transfer mechanism.

C. Simulation Approach

Due to the composite nature and double-wedge swept geometry of these fins, analytical solutions to the torsional stiffness of are difficult to calculate. Therefore, the finite element method provides a much more accurate and straightforward approach. The fin was modeled in ANSYS mechanical as a double-wedge geometry with a constant thickness-to-chord ratio. This resulted in a slight taper in thickness from the root to the tip, similar to the 3D-printed cores. The material assignments for the core and layup material were made using the values in Tables 1 and 2 respectively. Each woven carbon fiber ply was modeled in ACP Pre, ANSYS's composite toolbox, as two orthogonal unidirectional plies with half the thickness. This is because in the ACP Pre toolbox, "woven" fibers are treated as quasi-isotropic sheets, but this assumption is not quite valid since the twill sheets of prepreg used are only quasi-orthotropic along the fiber directions. The interlaminar stresses caused by the weave pattern were assumed to be negligible in order to take this approach.

The fin core geometry is similar to the geometry used to print the resin cores but with a few simplifying assumptions. The base fillet which connects the fin to the rocket was removed to simplify the meshing and remove the razor-thin areas at the edges. After the core volume and facesheet shells were meshed, the separate meshes were imported into a final static structural mechanical simulation, and attached using bonded multi-point constraint connections.

To set up the model, a fixed boundary was set on the core volume mesh at the root. At the tip, a moment was applied at the element faces that contacted the clamps in the experiment. Furthermore, a zero-displacement condition was added to the node in the center of the tip chord face. This prevented the translation of the node but allowed for free rotation. This additional constraint was added to ensure that the tip would rotate about the centroid of the tip cross-section, as was done in the experiment based on the clamp location. These conditions are shown in Fig. 5.

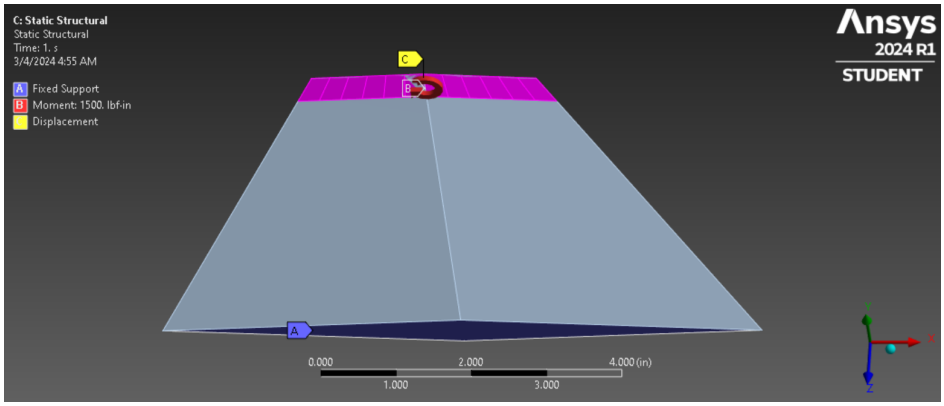

Fig. 5 Composite fin model in ANSYS with fixed boundary condition (A), moment load (B), and pinned node (C)

IV. Results and Discussion

A. Data Reduction

All the data was collected from the Instron load frame and ANSYS model. All data was reduced and analyzed using MATLAB.

In this experiment, the vertical force, F, and displacement, y, of the rack were directly measured. This raw data is shown in Fig. 6. The force applied by the load frame was converted to the equivalent torque applied to the clamp through the pinion (Eq. 1). The component of this moment in the radial direction of the fin calculated in Eq. 2, T_r, was used for for torsional stiffness calculations.

$$T = F \times d_p \tag{1}$$

$$T_r = T \cos\left(\tan^{-1}\left(\frac{\Delta r}{L_c}\right)\right) \tag{2}$$

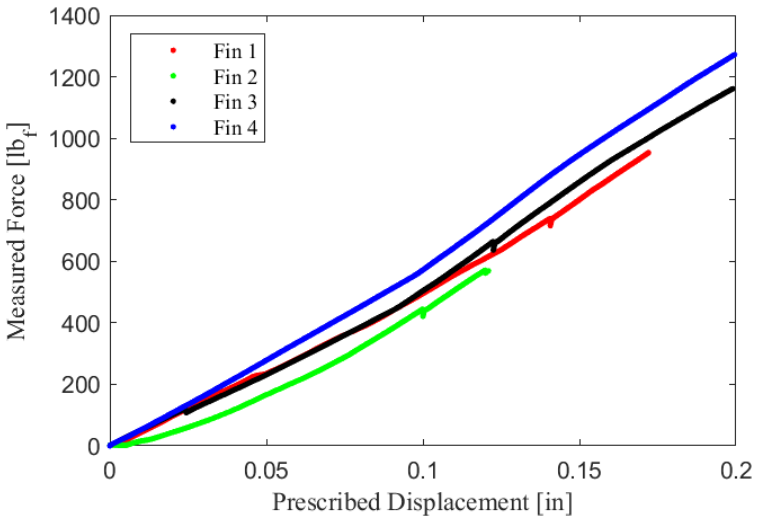

Fig. 6 The raw data for vertical force and displacement collected with the Instron load frame.

Additionally, the deformation of the test rig was considered to determine the true angular displacement of the fin. For this analysis, the torsional deformation of the square shaft was calculated (Eq. 3). The slope of the clamp plate deflection under the applied moment was also calculated to account for deformation in the clamp setup.

$$\phi_s = \frac{16TL_s}{2.25GA^2} \tag{3}$$

Where L_s is the length of the shaft, G is the shear modulus of A36 Steel, and A is the cross-sectional area of the square shaft. The latter term is a derivation of the polar moment of area for a square cross-section [16].

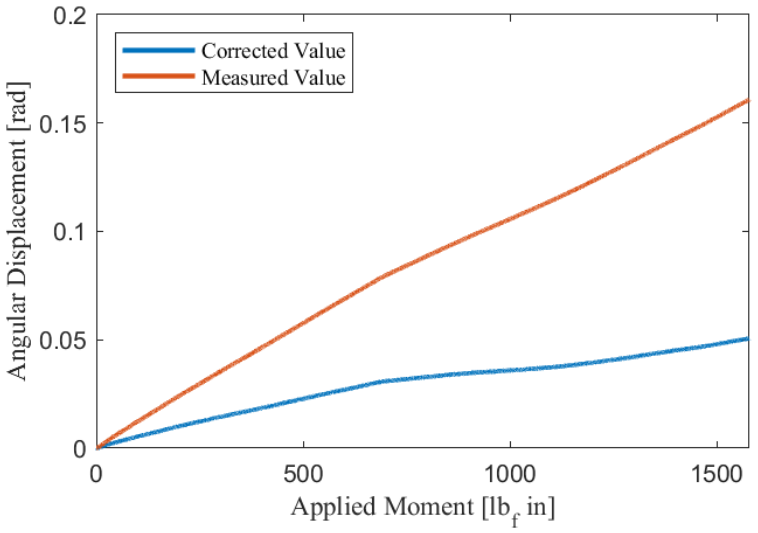

Fig. 7 Corrected angular displacement after accounting for rig deformation.

From this value, a small angle approximation was made to estimate the vertical displacement of the leading and trailing edges of the tip (Eq. 4).

$$\delta_t = \frac{c_t}{2}\left(\frac{2y}{d_p} - \phi_s\right) \tag{4}$$

These results were then compared to the simulated results from ANSYS. The total deformation for all elements from the static structural result was checked to ensure that the model behaved as intended. To determine the angular

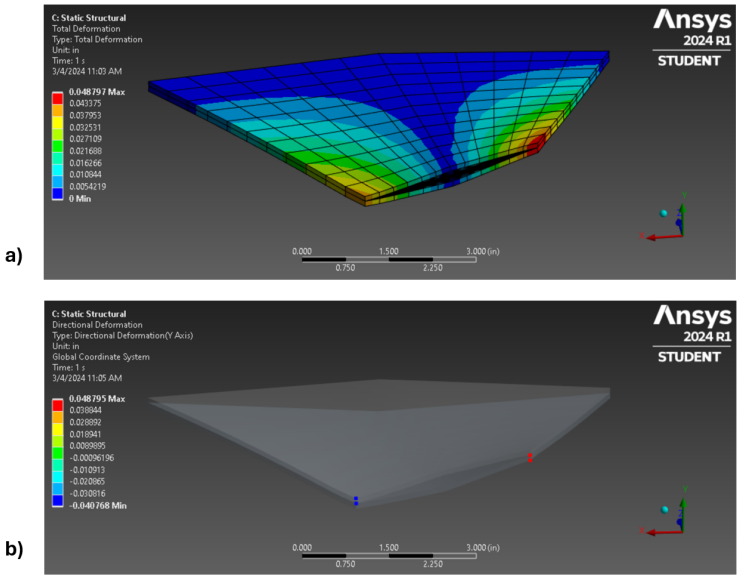

Fig. 8 Solution parameters retrieved from the ANSYS simulation: a) the total deformation and b) the vertical displacement at both tip edges.

displacement of the fin tip, the directional deformation in the fin's out-of-plane direction was retrieved. These results are shown in Fig. 8. A small angle approximation was made to determine the angular deformation of the modeled fin. Since the fin was designed as a perfectly elastic isotropic material, certain non-linear effects are not seen in the ANSYS model. A comparison of the experimental and simulated data is shown in Fig. 9.

B. Discussion

This testing showed a strong agreement between the ANSYS modeling and the actual torsional stiffness of a carbon fiber double-wedge fin. The fins had JG values ranging from $7.9 \times 10^4 lbf \cdot in^2$ at the lowest for the high temp resin core to $1.63 \times 10^5 lbf \cdot in^2$ for fin four which closely matches the ANSYS JG value of $1.76 \times 10^5 lbf \cdot in^2$. The High Temp resin is less stiff than the Rigid 10k so it is expected that it would have a lower torsional stiffness value when compared to a geometrically similar but materially different fin. This test also shows the effects of core material stiffness on JG with the tensile modulus of Rigid 10k being 3.6 times stiffer than the 2.75 GPa of High Temp. Unfortunately, no Poisson's ratio or shear modulus was given on the datasheet to better compare the elastic properties of these materials,

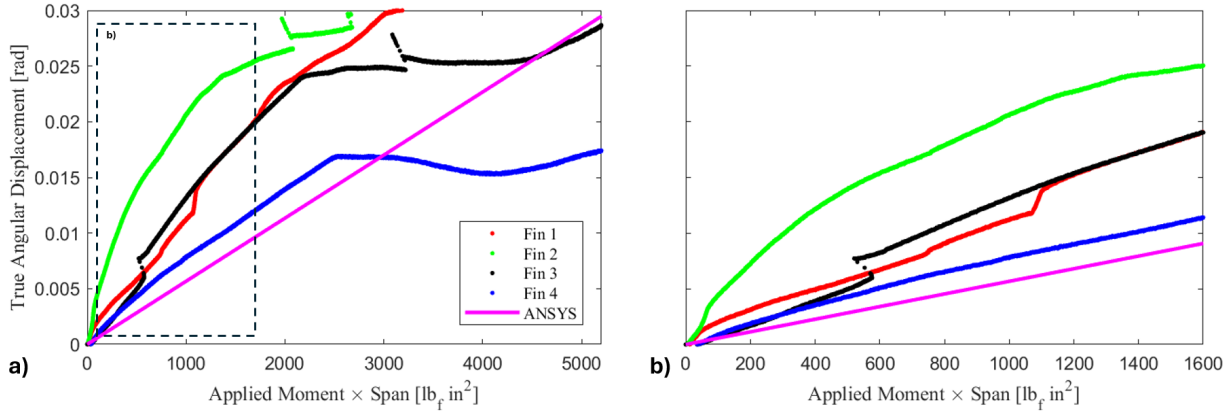

Fig. 9 a) The reduced data for each fin's tip displacement as a function of the applied moment, as well as the results from the ANSYS simulation; and b) a close-up of the linear regime of the data.

Fin	JG
1	$1.01 \times 10^5 lbf \cdot in^2$
2	$0.79 \times 10^5 lbf \cdot in^2$
3	$1.13 \times 10^5 lbf \cdot in^2$
4	$1.63 \times 10^5 lbf \cdot in^2$
ANSYS	$1.76 \times 10^5 lbf \cdot in^2$

Table 6 Fin JG values.

but the relatively small drop in JG (5%) for such a large change in elastic properties opens up the possibility for future lightweight and less stiff core constructions. Additionally, fins one and three, which broke off while bonding, show decreased but similar JG values of $1.01 \times 10^5 lbf \cdot in^2$ and $1.13 \times 10^5 lbf \cdot in^2$ at lower angular deformation. The fin with the best manufacturing technique and highest JG value is fin four which more closely follows the ANSYS data. The percent difference between the correctly manufactured fin four and the ANSYS results is 7.5% proving the validity of using ANSYS to design fins composite double-wedge to resist torsional flutter with a scaling factor applied. Even with less-than-ideal manufacturing techniques, this approach is valid, albeit with the factor of safety applied.

Some other interesting observations include the nonlinearity of JG with increased angular deflection. The JG value determined from the ANSYS is linear because this analysis assumed linear elastic deformation in the materials present. However, from the test data, there are two different regimes of torsional stiffness that occur as displacement increases. Below .02 radians of angular displacement for fin four and .027 radians for the other fins, the GJ value stays constant. However, at a certain point which differs for each fin the JG sharply increases before slowly dropping to its previous value. This behavior is reminiscent of strain hardening behavior, however, this could not have been caused by the carbon fibers or Rigid 10k since these materials do not have significant plastic deformation regions. Only the bulk properties of the prepreg carbon fiber were given and it may be possible that there is interlaminar strain hardening in the resin. It also could have been caused by play or deformation in the aluminum and steel test setup. Another note in the data is that the discontinuities seen in the data are caused by unloading and reloading the test setup. This was done to ensure the integrity of the test piece after cracking noises were heard.

V. Conclusion

In conclusion, this research paper presents a comprehensive investigation into the torsional stiffness of composite fins for sounding rockets, addressing the critical need for accurate characterization and validated modeling techniques in aerospace applications. By comparing experimental results with finite element analysis, the study successfully determined the torsional stiffness of composite fins, crucial for predicting and mitigating aeroelastic flutter.

Key findings from the experimental data revealed insights into the effects of core material stiffness and manufacturing techniques on torsional stiffness. The study highlighted the importance of material selection and manufacturing processes in optimizing the structural integrity and performance of composite fins. Moreover, the comparison between experimental and simulated data showcased the effectiveness of finite element analysis in predicting real-world behavior, facilitating the refinement of design iterations and optimization of composite structures.

While this study contributes to advancing the understanding of composite material behavior under torsional loading, further work is required to ensure that the approach is sound for different types of geometry. Additionally, future work may include developing different models to model the fins' torsional behavior. By integrating experimental testing with computational simulations, researchers can refine predictive models and optimize the design of composite structures, ensuring their resilience and efficacy in demanding flight environments.

Acknowledgments

The authors would like to extend their thanks to the Ramblin' Rocket Club and its project team Georgia Tech eXperimental Rocketry (GTXR) for providing the means and allowing this research to be done on their upcoming rocket's fins. The acknowledgments also extend to Georgia Tech's Student Government Association, the GT Aerospace Engineering Department, and the other club sponsors for making this research possible through financial contributions.

References

[1] Bae, J., Bae, J., Lee, I., and Lee, I., "Limit cycle oscillation of missile control fin with structural non-linearity," *Journal of Sound and Vibration*, 2004. https://doi.org/10.1016/s0022-460x(03)00125-1.

[2] Bauer, R., and Hardman, A., "Fin Flutter Analysis," 2013.

[3] Shubov, M. A., "Flutter phenomenon in aeroelasticity and its mathematical analysis," *Journal of Aerospace Engineering*, Vol. 19, No. 1, 2006, pp. 1–12.

[4] Bornassi, S., Bornassi, S., Navazi, H., Navazi, H., Haddadpour, H., and Haddadpour, H., "Aeroelastic instability analysis of a turbomachinery cascade with magnetorheological elastomer based adaptive blades," *Thin-walled Structures*, 2018. https://doi.org/10.1016/j.tws.2018.05.010.

[5] Bornassi, S., Bornassi, S., Navazi, H., Navazi, H., Haddadpour, H., and Haddadpour, H., "Coupled bending-torsion flutter investigation of MRE tapered sandwich blades in a turbomachinery cascade," *Thin-walled Structures*, 2020. https://doi.org/10.1016/j.tws.2020.106765.

[6] Theodorsen, T., Theodorsen, T., and Theodorsen, T., "General Theory of Aerodynamic Instability and the Mechanism of Flutter," 1934.

[7] Martin, D. J., and Martin, D. J., "Summary of flutter experiences as a guide to the preliminary design of lifting surfaces on missiles," 1958.

[8] Mallick, P. K., *Fiber-reinforced composites: Materials, manufacturing, and Design*, 3rd ed., CRC Press, 2008.

[9] Savoia, M., Savoia, M., Tullini, N., and Tullini, N., "Torsional response of inhomogeneous and multilayered composite beams," *Composite Structures*, 1993. https://doi.org/10.1016/0263-8223(93)90207-7.

[10] Garbowski, T., Garbowski, T., Gajewski, T., Gajewski, T., Grabski, J. K., and Grabski, J. K., "Torsional and Transversal Stiffness of Orthotropic Sandwich Panels," *Materials*, 2020. https://doi.org/10.3390/ma13215016.

[11] Armandei, M., Armandei, M., Fernandes, A. C., and Fernandes, A. C., "Torsional Instability of an Elastic Flat Plate due to Hydrodynamic Loads," *Journal of Mechanics*, 2014. https://doi.org/10.1017/jmech.2014.28.

[12] İbrahim Fadıl Soykök, Soykok, I. F., Ozcan, A. R., Ozcan, A. R., Taş, H., and Tas, H., "Evaluation of the failure responses of filament wound and pre-preg wrapped glass fiber/epoxy composite tubes under quasi-static torsional loading," *Materials Research Express*, 2019. https://doi.org/10.1088/2053-1591/ab0151.

[13] Astasari, A., Astasari, A., Sutikno, S., Sutikno, S., Wijanarko, W., and Wijanarko, W., "Bending and Torsional Characteristics of Carbon Fiber and Balsa Wood Sandwich Composite," *null*, 2016. https://doi.org/10.12962/j23546026.y2017i2.2270.

[14] Dea, S., Bresciani, C., Kumar, K., Murcin, N., Raaf, J., Ajluni, R., and Garud, P., "Shear Modulus Testing in Composite Sandwich Panels," *AIAA Region II Student Conference*, 2024.

[15] Garud, P., Johnson, C., and Lagares de Toledo, A., "Material Girl Launch Report," Tech. rep., Ramblin Rocket Club, 2024. URL rocketry.gatech.edu.

[16] Young, W. C., Budynas, R. G., and Sadegh, A. M., *Roark's formulas for stress and strain*, McGraw-Hill Education, 2012.